Applied Mathematics & Information Sciences **4**(2) (2010), 209–226
– An International Journal

Wave Propagation in Cylindrical Poroelastic Dry Bones

S. R. Mahmoud*
Mathematics Department, Faculty of Education, King Abdul Aziz University, K. S. A.
Email Address: srhassan@kau.edu.sa

Received June 22, 2008; Revised November 2, 2008

The wave propagation modeling in cylindrical human long dry bones with cavity is studied. The dynamic behavior of a dry long bones that has been modeled as a piezo-electric hollow cylinder of crystal class 6 is investigated. An analytic solutions for this mechanical wave propagation in a long dry bones have been obtained for the flexural vibrations. The frequency equation for poroelastic bones is obtained when the medium is subjected to certain boundary conditions. The dimensionless frequencies are calculated for poroelastic dry bones for various values for non-dimensional wave length. The generated electro-magnetic fields as a function of cylindrical coordinates are obtained and then the components of the magnetic field, which is due to the wave propagation in bones. The numerical results obtained have been illustrated graphically.

Keywords: Elastic, bones, poroelastic, transversely isotropic, mechanical wave, frequency equations.

1 Introduction

The Study of wave propagation over a continuous media is of practical importance in the field of engineering, medicine and in bi- engineering. Application of the poroelastic materials in medicinal fields such as orthopedics, dental and cardiovascular is well known [1]. In orthopedics wave propagation over bone is used in monitoring the rate of fracture heating, there are two types of osseous tissue such as cancellous or trabecular and compact or cortical bone, which are of different materials, with respect to their mechanical behavior. In macroscopic terms the percentage of porosity in the cortical bone is 3-5 , where as in the trabecular or cancellous the percentage of porosity is up to 90, [2]. The dynamic behavior method such as wave propagation and vibration of bone is necessary in measuring in vivo properties of bone by the above non- invasive method [3], papathanasopoulou, *et al.* [4] investigated. A theoretical analysis of the internal bone remodeling process induced by a medullar pin is presented, Fotiadis, *et al.* [5] studied wave propagation in human long dry

*Permanent address: Mathematics Department, Faculty of Science, University of Sohag, Egypt.

bones of arbitrary cross-section. Fotiadis *et al.* [6] presented wave propagation modeling in human long dry bones. Sebaa *et al.* [7] considered application of fractional calculus to ultrasonic wave propagation in human cancellous bone. Padilla, *et al.* [8] studied numerical of wave propagation in cancellous bone. Haiat *et al.* [9] investigated numerical simulation of the dependence of quantitative ultrasonic parameters on trabecular bone micro architecture and elastic constants. Pithious [10] presented, an alternative ultrasonic method for measuring the elastic properties of cortical bone. Kaczmarek *et al.* [11] investigated short ultrasonic waves in cancellous bone. Levitsky, *et al.* [12] studied wave propagation in cylindrical viscous layer between two elastic shells. Tadeu *et al.* [13] studied 3D elastic wave propagation modeling in the presence of 2D fluid-filled thin inclusions Dry bones are heterogeneous and an isotropic in nature. The bending waves which propagate along the cylinder causes an electrical field and hence a magnetic field. In the present paper, the three-dimensional equations of elastodynamics for transversely isotropic media are solved in terms of three displacement potentials, each satisfying a partial differential equation of the second order. For the hollow circular cylinder, subjected to certain boundary conditions (fixed and mixed boundary conditions), result in a characteristic frequency equation in determinantal form of the sixth order. Several special cases of the general frequency equation are discussed, including axially symmetric wave motion, the limiting modes of infinite wavelength, and longitudinal waves in a long thin solid cylinder. The analytical solution for the electro-mechanical wave propagation in a long bone has been obtained for the flexural vibration. The analysis presented here parallels the work of Fotiadis *et al.* [6] who studied the corresponding problem for hollow transversely isotropic circular cylinders. The numerical results obtained have been illustrated graphically.

2 Formulation of the Problem

Let us consider a transversely isotropic hollow cylinder, which is a geometric approximation to a long bone , it is defined in cylindrical coordinates r, θ, z. The long axis of the cylinder is assumed as the z axis and the inner and outer radii are termed as a and b. The linear theory of transverse isotropy elasticity, which is valid for small strains, gives the following stress displacements relations [6].

$$\begin{aligned}
\tau_{rr} &= C_{11}u'_{r,r} + C_{12}r^{-1}(\acute{u}_{\theta,\theta} + u_r\prime) + C_{13}u'_{z,z} + e_{13}V'_{,z} \\
\tau_{\theta\theta} &= C_{12}\tfrac{\partial u}{\partial r} + C_{11}r^{-1}\left(u + \tfrac{\partial v}{\partial \theta}\right) + C_{13}\tfrac{\partial w}{\partial z}, \\
\tau_{zz} &= C_{13}\left[\tfrac{\partial u}{\partial r} + r^{-1}\left(u + \tfrac{\partial v}{\partial \theta}\right)\right] + C_{33}\tfrac{\partial w}{\partial z}, \\
\tau_{rz} &= C_{44}[u'_{\theta,z} + u'_{z,r}] +, \, e_{15}V'_{,z'} - e_{14}\,r^{-1}\,V'_{,\theta} \\
\tau_{z\theta} &= C_{44}\left[\tfrac{\partial v}{\partial z} + r^{-1}\tfrac{\partial w}{\partial \theta}\right], \\
\tau_{r\theta} &= C_{66}[u'_{\theta,r} + r^{-1}\acute{u}_{r,\theta} - r^{-1}u_\theta\prime],
\end{aligned} \tag{2.1}$$

where $T'_{rr}, T'_{r\theta}$ and T'_{rz} are components of the stress tensor which satisfy the constitutive relations.

The system under consideration consists of a hollow piezoelectric circular cylinder of crystal class 6 with inner radius a and the outer one b The cylindrical polar system (r, ϕ, z) is introduced and the z-axis of the cylinder is assumed to be perpendicular to the isotropic plane of the medium. For a piezoelectric material of crystal class 6 the equations of motion and the equation of Gauss in cylindrical coordinates are given as

$$\begin{aligned} &C_{11}(u_{r,rr} + r^{-1}u_{r,r} - r^{-2}u_r) + C_{66}r^{-2}u_{r,\theta\theta} + C_{44}u_{r,z'z'} \\ &+ (C_{66} + C_{12})r^{-1}u_{\theta,r\theta} - (C_{66} + C_{11})r^{-2}u_{\theta,\theta} + (C_{44} + C_{13})u_{z,r\acute{z}} \\ &+ (e_{15} + e_{31})\acute{V}_{z,r\acute{z}} - e_{14}r^{-1}\acute{V}_{,\theta\acute{z}} = Qs\frac{\partial^2 u\theta'}{\partial t'^2} \end{aligned} \tag{2.2}$$

$$\begin{aligned} &(C_{66} + C_{12})r^{-1}u_{r,r\theta} + (C_{66} + C_{11})r^{-2}u_{r,\theta} + C_{66}(u_{\theta,rr} + r^{-1}u_{\theta,r} - r^{-2}u_{\theta'}) \\ &+ C_{11}r^{-2}u_{\theta,\theta\theta} + C_{44}u_{\theta,\acute{z}\acute{z}} + (C_{44} + C_{13})r^{-1}u_{z,\theta z'} + e_{14}V'_{,rz'} \\ &+ (e_{15} + e_{31})r^{-1}V'_{,\theta z'} = Qs\frac{\partial^2 u\theta'}{\partial t'^2}, \end{aligned} \tag{2.3}$$

$$\begin{aligned} &(C_{44} + C_{13})(u_{r,rz'} + r^{-1}u_{r,z'} + r^{-1}u_{\theta,\theta z'}) + C_{44}(u_{z,rr} + r^{-1}u_{z,\theta\theta}) \\ &+ C_{33}u_{z,z'z'} + e_{15}V'_{,rr} + r^{-1}V'_{,r} + r^{-2}V'_{\theta,\theta}) + e_{33}V'_{,z'z'} = Qs\frac{\partial^2 u_{z'}}{\partial t'^2}, \end{aligned} \tag{2.4}$$

$$\begin{aligned} &\in_{11} V'_{,rr} + r^{-1}V'_{,r} + r^{-2}V'_{,\theta\theta}) + \in_{33} V'_{,z'z'} - (e_{15} + e_{31})(u_{r,rz'} + r^{-1}u_{r,z'} + r^{-1}u_{\theta,\theta z'}) \\ &+ e_{14}(r^{-1}u_{r,\theta z'} - u_{\theta,rz'} - r^{-1}u_{\theta,z'}) - e_{15}(u_{z,rr} + r^{-1}u_{z,r} + r^{-1}u_{z,\theta\theta}) - e_{33}u_{z,z'z'} = 0, \end{aligned} \tag{2.5}$$

where $u_{r'}$, u_θ and $u_{z'}$ are the elastic displacement components, V' is the electrostatic potential, c_{ij} are the elastic constants, e_{ij} are the piezoelectric constants, $\in_{ij}$ are the dielectric permittivities, Qs is the mass density and $u_{ij} = \partial u_i/\partial x_j$. The boundary conditions are

$$\tau_{rr} = \tau_{rz} = \tau_{r\theta} = V' = 0, \qquad \text{at} \quad r = a,\, b \tag{2.6}$$

where $\tau_{rr},\ \tau_{r\theta}$ and τ_{rz} are components of the stress tensor which satisfy the constitutive relations

$$\begin{aligned} \tau_{rr} &= C_{11}u_{r,r} + C_{12}r^{-1}(u_{\theta,\theta} + u_r) + C_{13}u_{z,z} + e_{13}V'_{,z} \\ \tau_{r\theta} &= C_{66}[u_{\theta,r} + r^{-1}u_{r,\theta} - r^{-1}u_\theta] \\ \tau_{rz} &= C_{44}[u_{\theta,z} + u_{z,r}] + e_{15}V'_{,z'} - e_{14}\,r^{-1}\,V'_{,\theta.} \end{aligned} \tag{2.7}$$

The boundary conditions (2.6) correspond to the solution where the inner and the outer surface of the cylinder are Fixed of traction and coated with electrodes which are shorted.

3 Solution of the Problem

We introduce the following dimensionless variables:

$$\chi = \frac{r}{R}, \qquad Z = \frac{Z}{R}, \qquad u_\chi = \frac{1}{R}u'_r, \quad u_\theta = \frac{1}{R}u'_\theta, \quad u_z = \frac{1}{R}u'_z,$$

$$V = \frac{e_{33}}{Rc_{44}}V', \quad \check{C}_{ij} = \frac{c_{ij}}{c_{44}}, \ \hat{e}_{ij} = \frac{e_{ij}}{e_{33}}, \qquad \epsilon_{i3}^2 = \frac{e_{33}^2}{c_{44}\ \epsilon_{ii}}, \ t = \frac{1}{R}\sqrt{\frac{c_{44}}{Qs}}t',$$

where $R = r_1 - r_0$. To study the propagation of harmonic waves in the z' direction , we assume a solution of the form

$$\begin{aligned} u_\chi &= \left(G_{,\chi} + \frac{1}{\chi}\psi_{,\theta}\right)e^{i(\lambda z - \Omega t)}, \\ u_\theta &= \left(\frac{1}{\chi}G_{,\theta} - \psi_{,\chi}\right)e^{i(\lambda z - \Omega t)}, \\ u_z &= iwe^{i(\lambda z - \Omega t)}, \\ V &= i\phi e^{i(\lambda z - \Omega t)}, \end{aligned} \tag{3.1}$$

where G, ψ, ω and ϕ are functions of χ and $\theta, \Omega^2 = (R\omega)^2 Qs/c_{44}, \omega$ is the angular frequency, $\lambda = R\gamma$, and γ is the wave number. Using (9) the system (1)-(4) can be simplified as

$$D\begin{bmatrix} G \\ \psi \\ \omega \\ \phi \end{bmatrix} \equiv \begin{bmatrix} \check{C}_{11}\nabla^2 + \Omega^2 - \lambda^2 & 0 & -\lambda(1+\check{C}_{13}) & -\lambda(1+\check{e}_{15}+\check{e}_{31}) \\ 0 & \check{C}_{66}\nabla^2 + \Omega^2 - \lambda^2 & 0 & \lambda\check{e}_{14} \\ \lambda(1+\check{C}_{13})\nabla^2 & 0 & \nabla^2 + \Omega^2 - \check{C}_{33}\lambda^2 & \check{e}_{15}\nabla^2 - \lambda^2 \\ -\lambda(\check{e}_{15}+\check{e}_{31})\nabla^2 & \lambda\check{e}_{14}\nabla^2 & -(\check{e}_{15}\nabla^2 - \lambda^2) & \epsilon_{13}^{-2}\nabla^2 - \epsilon_{33}^{-2}\lambda^2 \end{bmatrix} \begin{bmatrix} G \\ \psi \\ \omega \\ \phi \end{bmatrix} = 0, \tag{3.2}$$

where

$$\nabla^2 \equiv \frac{\partial^2}{\partial\chi^2} + \frac{1}{\chi}\frac{\partial}{\partial\chi} + \frac{1}{\chi^2}\frac{\partial^2}{\partial\theta^2}.$$

To get the final solutions of the equations (3.2), using the method described in [5,6], we

obtain

$$
\begin{aligned}
u_z &= \sum_{j=1}^{4}\sum_{l=1}^{2}\Big\{\Big[\alpha_j{}^{m,1}\delta_j{}^{p^1}\frac{\partial}{\partial\chi}\zeta^{m,1}(k_j\chi)+\beta_j{}^{m,1}\delta_j{}^{p^2}\frac{m}{\chi}\zeta^{m,1}(k_j\chi)\Big]\cos(m\theta)\\
&\quad+\Big[-\alpha_j{}^{m,2}\delta_j{}^{p^1}\frac{m}{\chi}\zeta^{m,1}(k_j\chi)+\beta_j{}^{m,1}\delta_j{}^{p^1}\frac{\partial}{\partial\chi}\zeta^{m,1}(k_j\chi)\Big]\sin(m\theta)\Big\}e^{i(\lambda z-\Omega t)},\\
u_\theta &= \sum_{j=1}^{4}\sum_{l=1}^{2}\Big\{\Big[-\alpha_j{}^{m,1}\delta_j{}^{p^2}\frac{\partial}{\partial\chi}\zeta^{m,1}(k_j\chi)+\beta_j{}^{m,1}\delta_j{}^{p^1}\frac{m}{\chi}\zeta^{m,1}(k_j\chi)\Big]\cos(m\theta)\\
&\quad-\Big[\alpha_j{}^{m,1}\delta_j{}^{p^1}\frac{m}{\chi}\zeta^{m,1}(k_j\chi)+\beta_j{}^{m,1}\delta_j{}^{p^2}\frac{\partial}{\partial\chi}\zeta^{m,1}(k_j\chi)\Big]\sin(m\theta)\Big\}e^{i(\lambda z-\Omega t)},\\
u_z &= i\sum_{j=1}^{4}\sum_{l=1}^{2}\Big\{\Big[-\alpha_j{}^{m,1}\delta_j{}^{p^3}\frac{\partial}{\partial\chi}\zeta^{m,1}(k_j\chi)\Big]\cos(m\theta)\\
&\quad+\Big[\beta_j{}^{m,1}\delta_j{}^{p^3}\zeta^{m,1}(k_j\chi)\Big]\sin(m\theta)\Big\}e^{i(\lambda z-\Omega t)},\\
V &= i\sum_{j=1}^{4}\sum_{l=1}^{2}\Big\{\Big[\alpha_j{}^{m,1}\delta_j{}^{p^4}\zeta^{m,1}(k_j\chi)\Big]\cos(m\theta)\\
&\quad+\Big[\beta_j{}^{m,1}\delta_j{}^{p^4}\zeta^{m,1}(k_j\chi)\Big]\sin(m\theta)\Big\}e^{i(\lambda z-\Omega t)},
\end{aligned}
\tag{3.3}
$$

where

$$\delta_j{}^{pq}=-d_j{}^{pq}\,k_j^6+d_2{}^{pq}\,k_j^4-d_3{}^{pq}\,k_j^2+d_4{}^{pq},\quad p,q,j=1,2,3,4.$$

The stresses given by the constitutive equations (1) are expressed as:

$$
\begin{aligned}
T_{\chi\chi} &= \sum_{j=1}^{4}\sum_{l=1}^{2}\Big\{\Big[\alpha_j{}^{m,1}p_{pj}^{m,1}(k_j\chi)+\beta_j^{m,1}Q_{pj}^{m,1}(k_j\chi)\Big]\cos(m\theta)\\
&\quad+\Big[-\alpha_j{}^{m,1}Q_{pj}^{m,1}(k_j\chi)+\beta_j^{m,1}p_{pj}^{m,1}(k_j\chi)\Big]\sin(m\theta)\Big\}e^{i(\lambda z-\Omega t)},\\
T_{\chi\theta} &= \check{C}66\sum_{j=1}^{4}\sum_{l=1}^{2}\Big\{\Big[\alpha_j{}^{m,1}R_{pj}^{m,1}(k_j\chi)+\beta_j^{m,1}S_{pj}^{m,1}(k_j\chi)\Big]\cos(m\theta)\\
&\quad+\Big[-\alpha_j{}^{m,1}S_{pj}^{m,1}(k_j\chi)+\beta_j^{m,1}R_{pj}^{m,1}(k_j\chi)\Big]\sin(m\theta)\Big\},\\
T_{\chi z} &= i\sum_{j=1}^{4}\sum_{l=1}^{2}\Big\{\Big[\alpha_j{}^{m,1}T_{pj}^{m,1}(k_j\chi)+\beta_j^{m,1}U_{pj}^{m,1}(k_j\chi)\Big]\cos(m\theta)\\
&\quad+\Big[-\alpha_j{}^{m,1}U_{pj}^{m,1}(k_j\chi)+\beta_j^{m,1}T_{pj}^{m,1}(k_j\chi)\Big]\sin(m\theta)\Big\},
\end{aligned}
\tag{3.4}
$$

where the quantities $P_{pj}^{m,1}, Q_{pj}^{m,1}, R_{pj}^{m,1}, S_{pj}^{m,1}, T_{pj}^{m,1}$, and $U_{pj}^{m,1}$ are given in Appendix C of [6]. Replacing the expressions (3.3) and (3.4) into the boundary conditions (2.5), we obtain an algebraic system with 16 unknowns,which can be written as

$$Ax=0. \tag{3.5}$$

In order for the system (3.5) to have a nontrivial solution, the determinant of matrix A must vanish, that is,

$$det(A_{rs}) = 0, \qquad r, s = 1, 2, \ldots, 16. \tag{3.6}$$

This condition provides the frequency equation, the roots of which are the frequency coefficients $\Omega_{m,p}(\lambda)$, $m = 1, 2, \ldots, p = 1, 2, 3, 4$ of the system under discussion. The elements of the determinant (3.6) are given in [6].

4 Special Cases of the Mechanical Equations

4.1 The electrostatic potential is neglected

Let us assume the electrostatic potential V' is zero. Then the linear theory of transverse isotropy elasticity, which is valid for small strains and gives the following stress displacements relations [1].

$$\begin{aligned}
\tau_{rr} &= C_{11}\frac{\partial u_r}{\partial r} + C_{12}r^{-1}\left(u_r + \frac{\partial u_\theta}{\partial \theta}\right) + C_{13}\frac{\partial u_z}{\partial z},\\
\tau_{r\theta} &= C_{66}\left[\frac{\partial u_\theta}{\partial r} + r^{-1}\left(\frac{\partial u_r}{\partial \theta} - u_\theta\right)\right],\\
\tau_{rz} &= C_{44}\left[\frac{\partial u_z}{\partial r} + \frac{\partial u_r}{\partial z}\right],
\end{aligned} \tag{4.1}$$

where u_r, u_θ and u_z are the components of the displacement in the radial, circumferential, and axial directions; $C_{11}, C_{12}, C_{13}, C_{33}, C_{44}$ and C_{66} are the elasticconstants in the transversely isotropic case. The elastic constant C_{66} can be written in the form

$$C_{66} = \frac{1}{2}(C_{11} - C_{12}).$$

The mechanical field equations by using the three-dimensional stress equations of motion are

$$\begin{aligned}
\frac{\partial \sigma_{rr}}{\partial r} + r^{-1}\frac{\partial \tau_{r\theta}}{\partial \theta} + \frac{\partial \tau_{rz}}{\partial z} + r^{-1}(\sigma_{rr} - \sigma_{\theta\theta}) &= \rho\frac{\partial^2 u_r}{\partial t^2},\\
\frac{\partial \tau_{r\theta}}{\partial r} + r^{-1}\frac{\partial \sigma_{\theta\theta}}{\partial \theta} + \frac{\partial \tau_{\theta z}}{\partial z} + 2r^{-1}\tau_{\theta r} &= \rho\frac{\partial^2 u_\theta}{\partial t^2},\\
\frac{\partial \tau_{rz}}{\partial r} + r^{-1}\frac{\partial \tau_{\theta z}}{\partial \theta} + \frac{\partial \sigma_{zz}}{\partial z} + r^{-1}\tau_{\theta r} &= \rho\frac{\partial^2 u_z}{\partial t^2},
\end{aligned} \tag{4.2}$$

where ρ is the density and t is the time.

Substituting from equations (4.1) into the equation (4.2) leads to the following field

equations in terms of displacements

$$\begin{aligned}
C_{11}\Big[\frac{\partial^2 u_r}{\partial r^2}+r^{-1}\frac{\partial u_r}{\partial r}-r^{-2}u_r\Big]+r^{-2}C_{66}\frac{\partial^2 u_r}{\partial\theta^2}+C_{44}\frac{\partial^2 u_r}{\partial z^2}\\
+r^{-1}\left(C_{12}+C_{66}\right)\frac{\partial^2 u_\theta}{\partial\theta\partial r}-r^{-2}\left(C_{11}+C_{66}\right)\frac{\partial u_\theta}{\partial\theta}+\left(C_{13}+C_{44}\right)\frac{\partial^2 u_z}{\partial r\partial z}=\rho\frac{\partial^2 u_r}{\partial t^2},\\
r^{-1}\left(C_{12}+C_{66}\right)\frac{\partial^2 u_r}{\partial\theta\partial r}+r^{-2}\left(C_{11}+C_{66}\right)\frac{\partial u_r}{\partial\theta}+C_{66}\Big[\frac{\partial^2 u_\theta}{\partial r^2}+r^{-1}\frac{\partial u_\theta}{\partial r}-r^{-2}u_\theta\Big]\\
+r^{-2}C_{66}\frac{\partial^2 u_\theta}{\partial\theta^2}+C_{44}\frac{\partial^2 u_\theta}{\partial z^2}+r^{-1}\left(C_{13}+C_{44}\right)\frac{\partial^2 u_z}{\partial\theta\partial z}=\rho\frac{\partial^2 u_\theta}{\partial t^2},\\
\left(C_{13}+C_{44}\right)\frac{\partial^2 u_r}{\partial r\partial z}+r^{-1}\left(C_{13}+C_{44}\right)\frac{\partial u_r}{\partial z}+r^{-1}\left(C_{13}+C_{44}\right)\frac{\partial^2 u_\theta}{\partial\theta\partial z}\\
+C_{44}\left[\frac{\partial^2 u_z}{\partial r^2}+r^{-1}\frac{\partial u_z}{\partial r}-r^{-2}\frac{\partial^2 u_z}{\partial\theta^2}\right]+C_{33}\frac{\partial^2 u_z}{\partial z^2}=\rho\frac{\partial^2 u_z}{\partial t^2}.
\end{aligned}\tag{4.3}$$

Harmonic wave in hollow cylinder of infinite extent can be obtained by using the following solutions of the field equations

$$\begin{aligned}
u_r&=\Big[\frac{\partial\Phi}{\partial r}+\frac{1}{r}\frac{\partial\Psi}{\partial\theta}\Big]\cos\left(\omega t+\alpha z\right),\\
u_\theta&=\Big[\frac{\partial\Phi}{\partial\theta}-\frac{\partial\Psi}{\partial r}\Big]\cos\left(\omega t+\alpha z\right),\\
u_z&=\zeta\sin(\omega t+\alpha z),
\end{aligned}\tag{4.4}$$

where ω is the angular frequency and α is the wave number. Φ, Ψ, and ζ are displacement potentials which are introduced for facilitating the solution of the field equations (4.2). Substituting from the eqs. (4.4) into the eqs. (4.3), after regrouping them, leads to the following solution

$$\begin{aligned}
\Psi&=\left[A_1Z_n(\beta_1 r)+B_1W_n(\beta_1 r)\right]\sin n\theta,\\
\Phi&=\sum_{j=1}^{2}\left[A_{j+1}Z_n(\gamma_j r)+B_{j+1}W_n(\gamma_j r)\right]\cos n\theta,\\
\zeta&=\sum_{j=1}^{2}\left[A_{j+3}Z_n(\gamma_j r)+B_{j+3}W_n(\gamma_j r)\right]\cos n\theta.
\end{aligned}\tag{4.5}$$

The solutions of Φ and ζ are related to each other with the following relation

$$\Phi=g_j\left(r\right)\cos n\theta,\qquad \zeta=\frac{C_{11}P^2-\left(\rho\omega^2-C_{44}\alpha^2\right)}{\eta}\Phi,$$

where $\eta=\alpha\left(C_{13}+C_{44}\right)$ and $\alpha=2\pi/\lambda$, λ is the wave length.

Consider first solutions $\Psi\left(r,\theta\right)$ of the form $\Psi(r,\theta)=f(r)\sin(n\theta)$, where $n=0,1,2,3,\ldots$ are an integers indicating the numbers of circumferential waves, $g_j\left(r\right)=$

$A_{j+1}Z_n(\gamma_j r)+B_{j+1}Z_n(\gamma_j r)$ and $f(r)=A_1Z_n(\beta_1 r)+B_1W_n(\beta_1 r)$, where Z_n and W_n are respectively the Bessel functions and modified Bessel functions of order n [1].

Frequency equation

We use the following boundary conditions with inner surface and outer surface fixed.

$$\begin{aligned} u_r = u_\theta = u_z = 0 \qquad &\text{at} \quad r=a, \\ u_r = u_\theta = u_z = 0 \qquad &\text{at} \quad r=b. \end{aligned} \tag{4.6}$$

Substituting (3.2) and (3.1) into (4.6) and grouping the coefficients of $A_1, B_1A_2, B_{2,}A_3$ and B_3 lead to a determinant which is the characteristic frequency equation.

$$|a_{ij}|=0, \qquad (i,j=1,2,\ldots,6), \tag{4.7}$$

$$\begin{aligned}
a_{11} &= na^{-1}Z_n(\beta_1 a), & a_{12} &= na^{-1}W_n(\beta_1 a), \\
a_{13} &= \frac{n}{a}Z_n(\gamma_1 a)-\gamma_1\delta_1 Z_{n+1}(\gamma_1 a), & a_{14} &= \frac{n}{a}W_n(\gamma_1 a)-\gamma_1 W_{n+1}(\gamma_1 a), \\
a_{15} &= \frac{n}{a}Z_n(\gamma_2 a)-\gamma_2\delta_2 Z_{n+1}(\gamma_2 a), & a_{16} &= \frac{n}{a}W_n(\gamma_1 a)-\gamma_2 W_{n+1}(\gamma_2 a), \\
a_{21} &= \frac{n}{a}Z_n(\beta_1 a)-\beta_1\delta_2 Z_{n+1}(\beta_1 a), & a_{22} &= \frac{n}{a}W_n(\beta_1 a)-\beta_1 W_{n+1}(\beta_1 a), \\
a_{23} &= na^{-1}Z_n(\gamma_1 a), & a_{24} &= na^{-1}W_n(\gamma_1 a), \\
a_{25} &= na^{-1}Z_n(\gamma_2 a), & a_{26} &= na^{-1}W_n(\gamma_2 a), \\
a_{31} &= 0, & a_{32} &= 0, \\
a_{33} &= y_1 Z_n(\gamma_1 a), & a_{34} &= y_1 W_n(\gamma_1 a), \\
a_{35} &= y_2 Z_n(\gamma_2 a), & a_{36} &= y_2 W_n(\gamma_2 a), \\
a_{41} &= nb^{-1}Z_n(\beta_1 b), & a_{42} &= nb^{-1}W_n(\beta_1 b), \\
a_{43} &= \frac{n}{b}Z_n(\gamma_1 b)-\gamma_1\delta_1 Z_{n+1}(\gamma_1 b), & a_{44} &= \frac{n}{b}W_n(\gamma_1 b)-\gamma_1 W_{n+1}(\gamma_1 b), \\
a_{45} &= \frac{n}{b}Z_n(\gamma_2 b)-\gamma_2\delta_2 Z_{n+1}(\gamma_2 b), & a_{46} &= \frac{n}{b}W_n(\gamma_1 b)-\gamma_2 W_{n+1}(\gamma_2 b), \\
a_{51} &= \frac{n}{b}Z_n(\beta_1 b)-\beta_1\delta_2 Z_{n+1}(\beta_1 b), & a_{52} &= \frac{n}{b}W_n(\beta_1 b)-\beta_1 W_{n+1}(\beta_1 b), \\
a_{53} &= nb^{-1}Z_n(\gamma_1 b), & a_{54} &= nb^{-1}W_n(\gamma_1 b), \\
a_{55} &= nb^{-1}Z_n(\gamma_2 b), & a_{56} &= nb^{-1}W_n(\gamma_2 b), \\
a_{61} &= 0, & a_{62} &= 0, \\
a_{63} &= y_1 Z_n(\gamma_1 b), & a_{64} &= y_1 W_n(\gamma_1 b), \\
a_{65} &= y_2 Z_n(\gamma_2 b), & a_{66} &= y_2 W_n(\gamma_2 b).
\end{aligned}$$

As preciously stated, Z denotes a J or I functions, and W denotes a Y or K functions. The proper choice being given in Table 4.1 which shows bessel functions employed in various frequency ranges.

Table 4.1: Bessel functions employed in various frequency ranges.

Interval	f	g_1	g_2
$0 < \rho\omega^2 < \alpha^2 C_{44} < 1$	$I_n(\beta_1 r) K_n(\beta_1 r)$	$I_n(\gamma_1 r) K_n(\gamma_1 r)$	$I_n(\gamma_2 r) K_n(\gamma_2 r)$
$1 < \rho\omega^2/\alpha^2 C_{44} < C_{33}/C_{44}$	$J_n(\beta_1 r) Y_n(\beta_1 r)$	$I_n(\gamma_1 r) K_n(\gamma_1 r)$	$J_n(\gamma_2 r) Y_n(\gamma_2 r)$
$\rho\omega^2/\alpha^2 C_{44} > C_{33}/C_{44}$	$J_n(\beta_1 r) Y_n(\beta_1 r)$	$J_n(\gamma_1 r) Y_n(\gamma_1 r)$	$J_n(\gamma_2 r) Y_n(\gamma_2 r)$

Furthermore, the parameters δ_j assume the values ± 1 as outlined below.

$$\begin{aligned} \rho\omega^2 < \alpha^2 C_{44} \quad &: \qquad \delta_1 = -1 \quad \delta_2 = -1, \\ \alpha^2 C_{44} < \rho\omega^2 < \alpha^2 C_{33} \quad &: \qquad \delta_1 = -1 \quad \delta_2 = 1, \\ \rho\omega^2 > \alpha^2 C_{33} \quad &: \qquad \delta_1 = 1 \quad \delta_2 = 1. \end{aligned}$$

Note that, the value of these parameters is 1 when the Bessel functions J and Y are used and -1 when I and K are used. For known value of the elastic constants and given dimensions of the cylinder the frequency ϖ may be computed as a function of wavelength $\lambda, (\lambda = 2\pi/\alpha)$ from the characteristic eqs.(4.7) by an iteration procedure. Here in the present analysis we consider only the special cases of eqs. $(4.7$). Here we are just going to consider that lowest mode for $n = 1, 2$ which is the first flexural mode, this is an important mode for the experimental results. The determinant (4.7) which gives the relation between the wave length and the angular frequency is evaluated for different wave lengths.

4.2 Motion independent of z

As the wavenumber $\alpha \longrightarrow 0$ (i.e., for infinite wavelength, $\lambda = 2\pi/\alpha$), the following simplifications result: $\gamma_1 \longrightarrow \left[\frac{\rho w^2}{C_{11}}\right]^{1/2}$, $\gamma_2 \longrightarrow \left[\frac{\rho w^2}{C_{11}}\right]^{1/2}$,

$$\lambda_1 \alpha \longrightarrow -\alpha^2 (C_{44} + C_{13}) / \ (C_{11} - C_{44})$$

$$\lambda_2 \alpha \longrightarrow \rho\alpha^2 (C_{44} - C_{13}) / \ C_{44} (C_{11} + C_{44})$$

$$\alpha / (\lambda_2 - \alpha) \longrightarrow 0, \quad (\lambda_1 - \alpha) / (\lambda_2 - \alpha) \longrightarrow 0, \tag{4.2.1}$$

Hence $\alpha_{11} = 0 = \alpha_{22} = \alpha_{23} = \alpha_{24} = \alpha_{51} = \alpha_{52} = \alpha_{53} = \alpha_{54,}$and the characteristic eq. $(4.1.7)$ fixed boundary conditions may be written as the product of two determinants

$$\Delta_1 \Delta_2 = 0 \tag{4.2.2}$$

$$\Delta_1 = \begin{vmatrix} a_{11} & a_{12} & a_{13} & a_{14} \\ a_{31} & a_{31} & a_{31} & a_{31} \\ a_{41} & a_{41} & a_{41} & a_{41} \\ a_{61} & a_{61} & a_{61} & a_{61} \end{vmatrix}, \quad \Delta_2 = \begin{vmatrix} a_{25} & a_{26} \\ a_{55} & a_{56} \end{vmatrix}$$

The elements a_{ij}-in equation $(4.2.2)$ are given by eq. $(4.1.7)$ fixed boundary conditions with $\alpha- > 0$ (i.e., for infinite wavelength, $\lambda = 2\pi/\alpha$) and the appropriate simplifications outlined in Eq. $(4.2.1)$. Furthermore, the Z and W are either J or Y functions, in accordance to table (4.1), since $\rho\varpi^2 > \alpha^2 C_{33}$, when $\alpha- > 0$. (i.e., for infinite wavelength, $\lambda = 2\pi/\alpha$).

The equation $\Delta_1 = 0$ corresponds to plane-strain vibrations and is equivalent to that for the isotropic cylinder, with the shear constant C_{44} being replaced by C_{66}. This is to be expected since the z axis is perpendicular to the plane of isotropy. The equation Δ_2 represents motion involving the axial displacement u_z only, corresponding to longitudinal-shear vibrations. This equation could have been obtained immediately from the displacement equations of equilibrium (2.2) by setting, $u_r = 0 = u_\theta$, $\frac{\partial}{\partial z} = 0$ with the result $C_{44}\left[\frac{\partial^2 u_z}{\partial r^2} + \frac{1}{r}\frac{\partial u_z}{\partial r} + \frac{1}{r^2}\frac{\partial^2 u_z}{\partial \theta^2}\right] = \rho\frac{\partial^2 u_z}{\partial t^2}$, subject to the boundary conditions $\frac{\partial u_z}{\partial r} = 0$ on $r = a, b$. It may be noted that the plane-strain and longitudinal-shear vibrations are uncoupled when $a = 0$ and become coupled for a nonzero wavenumber (i.e., for infinite wavelength, $\lambda = 2\pi/\alpha$). No further discussion of these frequency equations is necessary.

4.3 Motion independent of θ

For motion independent of θ (i.e., $n = 0$), the characteristic eqs. $(4.1.7)$ may again be represented as the product of two determinants $\Delta_3,\ \Delta_4$ where

$$\Delta_3\Delta_4 = 0 \tag{4.3.1}$$

The elements a_{ij}-in equation (4.3.1) are given by eq. $(4.1.7)$ fixed boundary conditions, with $n = 0$

$$\Delta_3 = \begin{vmatrix} a_{12} & a_{14} & a_{15} & a_{16} \\ a_{23} & a_{24} & a_{25} & a_{26} \\ a_{43} & a_{44} & a_{45} & a_{46} \\ a_{53} & a_{54} & a_{55} & a_{56} \end{vmatrix}, \quad \Delta_4 = \begin{vmatrix} a_{31} & a_{32} \\ a_{61} & a_{62} \end{vmatrix}$$

The frequency equation Δ_3 represents the coupled radial and axial motions, which are completely uncoupled from the pure torsional motions given by $\Delta_4 = 0$.These frequency equations have been computed approximately, for orthotropic thick shells, which includes transverse isotropy as a special case. The five elastic constants C_{ij} appear in Eq. $(4.3.1)$ However, this equation reduces to that of the special case of isotropy. For purely torsional modes,the frequency equation $\Delta_4 = 0$ reduces to $J_2(\beta_1 a)\,Y_2(\beta_1 b) - J_2(\beta_1 b)\,Y_2(\beta_1 a) = 0$, for $\rho\omega^2 < \alpha^2 C_{44}$ where $\beta_1 = \left|\frac{(\rho\omega^2 - C_{44}\alpha^2)}{C_{66}}\right|^{1/2}$. The corresponding frequency equation for $e < \rho\omega^2/C_{44}\alpha^2 < 1$ is given by $I_2(\beta_1 a)\,K_2(\beta_1 b) - I_2(\beta_1 b)\,K_2(\beta_1 a) = 0$,which has no real roots except the trivial solution. Thus, the phase velocity of torsional waves is always greater than or equal to $(C_{44}/\rho)^{1/2}$

4.4 Solid circular cylinder

So far, we have considered the frequency equations for various types of motions of hollow circular cylinders. It is a trivial matter to deduce from this analysis the corresponding frequency equations for a solid circular cylinder. In the latter case, the inner radius $a \longrightarrow 0$ and furthermore, the Bessel functions K and Y result in unbounded stresses and displacement at the origin $r = 0$. Hence all the coefficients a_{ij}- involving a and the W functions must vanish and the frequency equation for the solid circular cylinder reduces to

$$\Delta_5 = \begin{vmatrix} a_{41} & a_{43} & a_{45} \\ a_{51} & a_{53} & a_{55} \\ a_{61} & a_{63} & a_{65} \end{vmatrix} = 0, \quad \Delta_6 = \begin{vmatrix} a_{43} & a_{45} \\ a_{53} & a_{55} \end{vmatrix} = 0 \tag{4.4.1}$$

The elements a_{ij}-in $\Delta_5 = 0$ are given by eq. $(4.1.7)$ fixed boundary conditions, with $a = 0$, An interesting degenerate case of Δ_5 (Eq. 4.4.1) is that of axially symmetric motions (i.e., $n = 0$). The frequency equation for this type of motion reduces to $a_{43} = \frac{n}{b} Z_n(\gamma_1 b) - \gamma_1 \delta_1 Z_{n+1}(\gamma_1 b)$, $a_{45} = \frac{n}{b} Z_n(\gamma_2 b) - \gamma_2 \delta_2 Z_{n+1}(\gamma_2 b)$, $a_{53} = nb^{-1} Z_n(\gamma_1 b)$, $a_{55} = nb^{-1} Z_n(\gamma_2 b)$. If we assume now that the cross-sectional dimensions of the cylinder are small as compared to the length (i.e., $\gamma_1 b << 1,\ \gamma_2 b << 1$), an approximate value of the frequency of longitudinal waves in a bar can be obtained. Representing the Bessel functions in elements a_{ij} as power series in $\gamma_i b$, a detailed analysis indicates that this type of motion can occur only when the frequency ϖ lies in the interval $\alpha^2 C_{44} < \rho\varpi^2 < \alpha^2 C_{33}$ When first terms only are retained in the power series expansions, the frequency ϖ is approximated by the expression $\rho\varpi^2 = \alpha^2 C_{33} - \left[\left(\alpha^2 C_{13}^2\right) / (C_{11} - C_{66})\right]$. Thus, the velocity $(C = \varpi/\alpha)$ with which these waves are propagated along the bar is $C = \left[\left(C_{11}C_{33} - C_{66}C_{33}^2\right) / \rho (C_{11} - C_{66})\right]^{1/2}$. For the special case of the isotropic cylinder $C_{11} = C_{33}$, $C_{12} = C_{13}$, $C_{66} = C_{44} = (C_{11} - C_{12})/2$ and the velocity C becomes $C = \left[C_{44}(2C_{11} - 4C_{44}) / \rho (C_{11} - C_{44})\right]^{1/2}$. In terms of the Lame constants λ, μ, this expression reduces to $C = \left[\mu(3\lambda + 2\mu) / \rho(\lambda + \mu)\right]^{1/2} = (E/\rho)^{1/2}$where $\lambda + 2\mu = C_{11}$, $\mu = C_{44}$ and E is Young's modulus. This is the result in this investigations of longitudinal vibrations of bars. If more-accurate values of the frequency ϖ are desired, it would appear to be more efficient to go directly to the exact frequency equation $\Delta_6 = 0$ rather than perform the tedious analysis required in obtaining higher-order approximations in the manner outlined above.

5 Effect of electrostatic potential on magnetic field

Let us consider the electromagnetic field equations in Gaussian units:

$$\begin{array}{l} \vec{\nabla} \times \vec{H} = \frac{1}{C} \frac{\partial \vec{D}}{\partial t} + \frac{4\pi}{C} \vec{J}, \quad \vec{\nabla} \cdot \vec{B} = 0, \quad \vec{\nabla} \times \vec{E} = -\frac{1}{C} \frac{\partial \vec{B}}{\partial t}, \\ \vec{\nabla} \cdot \vec{D} = 4\pi q, \quad \vec{B} = \vec{H} + 4\pi \vec{M} \end{array} \tag{5.1}$$

where $\overrightarrow{H}, \overrightarrow{B}, \overrightarrow{M}, \overrightarrow{E}, \overrightarrow{D}, \overrightarrow{J}, q$ and C are the magnetic field intensity, the magnetic flux density, the magnetization vector, the electric field,the electric displacement vector, the total free current density, the total free charge density, and the velocity of light respectively. The operator is defined in terms of the unit vectors of the cylindrical coordinates (r, θ, z) . $\overrightarrow{\nabla} = \frac{\partial}{\partial r}\overrightarrow{e_r} + \frac{1}{r}\frac{\partial}{\partial r}\overrightarrow{e_\theta} + \frac{\partial}{\partial z}\overrightarrow{e_z}$. In the case of dry bone [1] $q = 0$, $\overrightarrow{J} = \overrightarrow{M} = \overrightarrow{0}$..Thus equations (5.1) become:

$$\overrightarrow{B} = \overrightarrow{H}, \quad \overrightarrow{\nabla} \times \overrightarrow{H} = \frac{1}{C}\frac{\partial \overrightarrow{D}}{\partial t}, \quad \overrightarrow{\nabla} \cdot \overrightarrow{D} = 0. \tag{5.2}$$

6 The solution of the vacuum

The inner (i) and the outer $(\circ)$ regions are going to be obtained from the following set:

$$\overrightarrow{\nabla} \times \overrightarrow{B} = \overrightarrow{0}, \qquad \overrightarrow{\nabla} \cdot \overrightarrow{B} = 0 \tag{6.1}$$

Assuming a solution for $\overrightarrow{B}$ of the following form:

$$\begin{aligned} B_r &= b_1(r)\, e^{in\theta} \sin(wt + \alpha z), \\ B_\theta &= b_2(r)\, e^{in\theta} \sin(wt + \alpha z), \\ B_z &= b_3(r)\, e^{in\theta} \cos(wt + \alpha z). \end{aligned} \tag{6.2}$$

and substituting in (6.1) yields the following set for the components of $\overrightarrow{B}$:

$$b_1 = \frac{1}{\alpha}\left[\frac{db_3(r)}{dr}\right], \quad b_2 = \frac{1}{\alpha}\frac{in}{r}b_3, \quad \frac{d^2b_3}{dr^2} + r^{-1}\frac{db_3}{dr} - \left[r^{-2}n^2 + \alpha^2\right]b_3 = 0. \tag{6.3}$$

Using the regularity conditions at $r = 0$ gives the solution for the inner of vacuum.

$$\begin{aligned} B_r^i &= A_9\left[I_{n+1}(\alpha r) + \frac{n}{r\alpha}I_n(\alpha r)\right] e^{in\theta} \sin(wt + \alpha z), \\ B_\theta^i &= A_9\frac{in}{r\alpha}I_n(\alpha r) \sin(wt + \alpha z), \\ B_z^i &= A_9 I_n(\alpha r) \cos(wt + \alpha z). \end{aligned} \tag{6.4}$$

7 Numerical Results and Discussion

The numerical results for the frequency equation are computed for the bone. Since the frequency equation is transcendental in nature, there are an infinite number of roots for the frequency equation. The results of frequency versus wavelength are plotted in Figs. (7.1)-(7.3) for bones (the transversely isotropic materials) for several values of n the number of circumferential waves. Each of Fig (7.1) and Fig (7.2) contains the first three modes obtained from the approximate theories. Note that, since the determinantal equations $(4.1.2)$ is transcendental in nature, there are an infinite number of modes for each value of $n = 1, 2, 3$. In most cases, the results of the approximate theory, indicated by the

frequency which it decreasing with increasing wavelength. It is notes the first mode of the frequency coincide with the second mode of the frequency in the range $35 \leq \lambda \leq 50$.The roots are obtained for the Flexural mode $n = 1, 2$ in the cases of fixed boundary condition and mixed boundary condition are plotted and presented in Fig. (7.3).

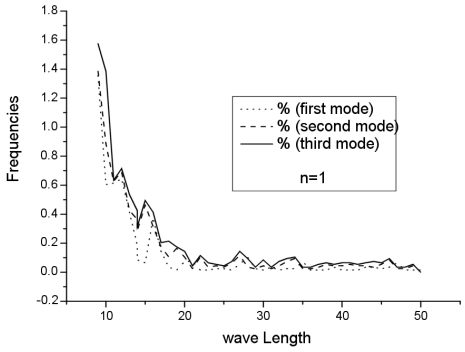

Figure 7.1: Frequency versus wavelength for $n = 1$.

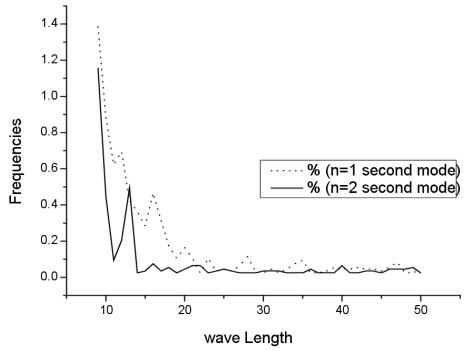

Figure 7.2: Frequency versus wavelength for $n = 2$.

The deviation of dispersion curves for the flexural modes are quite small at larger non-dimensional wavelength, but they almost coincide in the range $1 \leq \lambda \leq 33$. (in the fixed boundary condition). In mixed boundary condition the deviation of dispersion curves for the flexural modes are small at larger non-dimensional wavelength, but the deviation of dispersion curves for the flexural modes are large at smaller non-dimensional wavelength in the range $1 \leq \lambda \leq 23$.

Figs. $(7.4) - (7.9)$ show the components of the external magnetic induction $B_r,\ B_\theta$ and B_z with respect to the radius r, for different values of wavelengths, respectively. It is notice

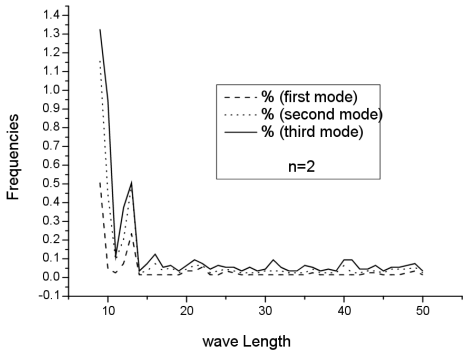

Figure 7.3: The dispersion curves of the poroelastic material for various n.

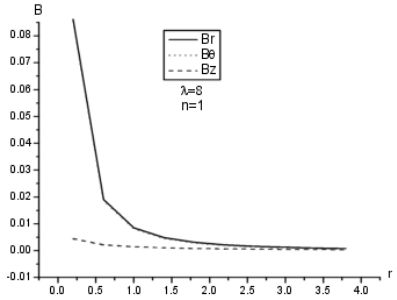

Figure 7.4: The variations of components of the external magnetic induction B_r, B_θ and B_z with respect to the radial r, for wavelengths $(\lambda = 8)$.

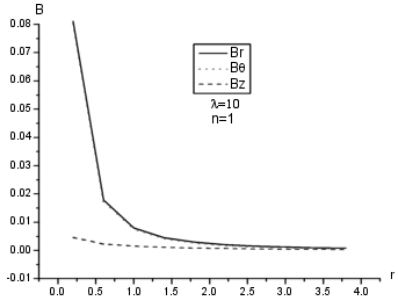

Figure 7.5: The variations of components of the external magnetic induction B_r, B_θ and B_z with respect to the radial r, for wavelengths $(\lambda = 10)$.

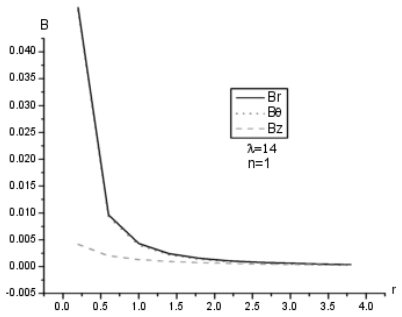

Figure 7.6: The variations of components of the external magnetic induction B_r, B_θ and B_z with respect to the radial r, for wavelengths $(\lambda = 14)$.

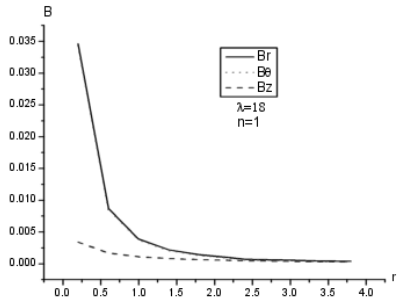

Figure 7.7: The variations of components of the external magnetic induction B_r, B_θ and B_z with respect to the radial r, for wavelengths $(\lambda = 18)$.

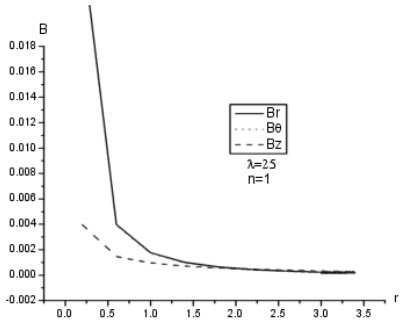

Figure 7.8: The variations of components of the external magnetic induction B_r, B_θ and B_z with respect to the radial r, for wavelengths $(\lambda = 25)$.

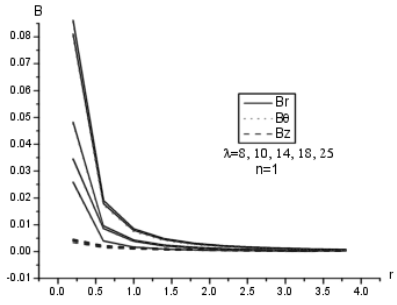

Figure 7.9: The variations of components of the external magnetic induction B_r, B_θ and B_z with respect to the radial r, for wavelengths $(\lambda = 8, 10, 14, 18, 25)$.

that the components of the external magnetic induction decrease with increasing of the radial r.

Table 7.1: Summary of the approximate geometry of the femur and the material constants in Gaussian units which are used in the computations, where, h is thickness of the cylinder $h = b - a$ where a is the inner radius, b is the outer radius and b/a is the ratio.

Elasticcoefficients [1]	Piezoelectriccoefficients [2]	Dielectriccoefficients [2]
$c_{11} = 2.12 \times 10^{10}$	$e_{31} = 1.50765 \times 10^{-3}$	$\epsilon_{11} = 88.54 \times 10^{-12}$
$c_{12} = 0.95 \times 10^{10}$	$e_{33} = 1.87209 \times 10^{-3}$	$\epsilon_{33} = 106.248 \times 10^{-12}$
$c_{13} = 1.02 \times 10^{10}$	$e_{14} = 17.88215 \times 10^{-3}$	
$c_{44} = 0.75 \times 10$	$e_{15} = 3.57643 \times 10^{-3}$	

Table 7.2: Frequency spectra for crystal class 6 hollow bones as a function of the ratio a/b.

No.	$a = 0$	$a/b = 0.21$	$a/b = 0.43$	$a/b = 0.57$	$a/b = 0.71$	$a/b = 0.86$
1	0.5736	0.4907	0.4130	0.3502	0.2760	.1021
2	0.9790	0.7912	0.6026	0.4771	0.3514	0.2257
3	1.3208	1.0598	0.7983	0.6237	0.4490	0.2746
4	1.4645	1.1810	0.8796	0.6897	0.5890	0.2955
5	1.4751	1.2892	0.9867	0.7651	0.4931	0.3216
6	1.6507	1 .4557	1.2168	1.7376	0.5437	0.3678
7	2.0530	1 .9534	1.9449		0.6588	0.3792

8 Conclusion

A characteristic frequency equation for the most general type of harmonic waves in a hollow circular cylinder of transversely isotropic material has been derived. This frequency equation must be separated into three frequency ranges because of the changing nature of the Bessel functions involved. As the wavelengths approaches infinity, the plane-strain vibrations become uncoupled from the longitudinal shear vibrations. These two types of motion become coupled for a non-infinity wavelengths. For flexural motions $(n = 1, 2)$, the coupled radial and axial motions are completely uncoupled from the pure torsional motions. When both the wavelength is infinity and $n = 1, 2$ the three displacement potential functions $f,\ g_1$ and g_2 generate three uncoupled families of modes that may be identified as plane-strain extensional, plane-strain shear, and longitudinal shear, respectively. The characteristic frequency equations $(4.1.2)$ for the hollow cylinder can readily be reduced to that for the solid cylinder on taking the limit $a \to 0$. Finally, the results for approximate frequency of longitudinal vibrations of a long solid bar obtained are generalized to the case of a transversely isotropic solid cylinder. The wave propagation in transversely isotropic cylinders, numerical results of the characteristic equation derived here are presented. Included in this presentation is a discussion of the variation of the frequency spectrum with the physical parameters. The dispersion curve for flexural mode $n = 1, 2$ deviate. The numerical results are given illustrated graphically for the magnetic field, which is due to the wave propagation in bones.

Acknowledgement

Special thanks are due to Professor A. M. Abd-Alla [1] for his helpful discussions and valuable remarks.

References

[1] A. M. El-Naggar, A. M. Abd. Alla and S. R. Mahmoud, Analytical solution of electromechanical wave propagation in long bones, *Appl. Math. Comput.* **119** (2001), 77–98.

[2] D. I. Fotiadis, G. Fouttsitzi, and C. V. Massalas, Wave propagation modeling in human long bones, *Acta Mech. Sin.* **137** (1999), 65–81.

[3] D. I. Fotiadis, G. Fouttsitzi, and C. V. Massalas, Wave propagation in human long bones of arbitrary cross section, *Int. J. Engng. Sci.* **38** (2000), 1553–1591.

[4] G. Haeat, F. Padilla, R. Barkmann, C. C. Gluer, and P. Laugier, Numerical simulation of the dependence of quantitative ultrasonic parameters on trabecular bone micro architecture and elastic constants, *Ultrasonic* **44** (2006), 289–294.

[5] J. M. Jurist, In vivo determination of the elastic response of bone. I. Method of ulnar resonant frequency determination, *Phys. Medical Biol.* **15** (1970), 417–426.

[6] M. Kaczmarek, J. Kubik, and M. Pakula, Short ultrasonic waves in cancellous bone, *Ultrasonic* **40** (2002), 95–100.

[7] S. P. Levitsky, R. M. Bergman, and J. Haddad, Wave propagation in a cylindrical viscous layer between two elastic shells, *Int. J. Engng. Sci.* **42** (2004), 2079–2086.

[8] A. N. Natali and E. A. Meroi, A review of the biomechanical properties of bone as a material, *J. Biomed. Engng.* **11** (1989), 266–276.

[9] F. Padilla, E. Bossy, G. Haiat, F. Jenson, and P. Laugier, Numerical simulation of wave propagation in cancellous bone, ultrasonic propagation in cancellous bone, *Ultrasonic* **44** (2006), 239–243.

[10] V. A. Papathanasopoulou, D. I. Fotiadis, G. Foutsitzi, and C. V. Massalas, A poroelastic bone model for internal remodeling, *Int. J. Engng. Sci.* **40** (2002), 511–530.

[11] M. Pithious, P. Lasaygues, and P. Chabrand, An alternative ultrasonic method for measuring the elastic properties of cortical bone, *J. of Biomechanics* **35** (2002), 961–968.

[12] N. Sebaa, Z. E. A. Fellah, W. Lauriks, and C. Depollier, Application of fractional calculus to ultrasonic wave propagation in human cancellous bone, *Signal Processing* **10** (2006), 2668–2677.

[13] A. Tadeu, P. Mendes, and J. Anto, 3D elastic wave propagation modelling in the presence of 2D fluid-filled thin inclusions, *Engineering Analysis with Boundary Elements* **30** (2006), 176–193.

Samy Refahy Mahmoud Hassan was born in Egypt. He received his Ph.D. from Faculty of Science Sohag - South Valley University in 2004. His dissertation title is “Geometry of Gauss maps for manifolds in Euclidean Spaces”. His current research interests include Theory of Elasticity and Thermoelasticity and Wave Propagation. He has published many papers in international refereed journals and authored two books.